Supplemental Document

Emergent optical nonreciprocity and chirality-controlled magneto-optical resonance in a hybrid magneto–chiral metamaterial: supplement

PEISONG PENG,[1] GRIJA THAPA,[2] JIANGFENG ZHOU,[2,3] AND DIYAR TALBAYEV[1,*]

[1] *Department of Physics and Engineering Physics, Tulane University, 6400 Freret St., New Orleans, Louisiana 70118, USA*
[2] *Department of Physics, The University of South Florida, 4202 East Fowler Avenue, Tampa, Florida 33620-7100, USA*
[3] *e-mail: jiangfengz@usf.edu*
[*] *Corresponding author: dtalbaye@tulane.edu*

Supplement DOI: https://doi.org/10.6084/m9.figshare.21751358

Parent Article DOI: https://doi.org/10.1364/OPTICA.480791

Emergent optical nonreciprocity and chirality-controlled magneto-optical resonance in a hybrid magneto-chiral metamaterial: supplemental document

1. Calculation of Faraday rotation and Faraday ellipticity for a uniform slab of InSb

We perform this calculation using the circular eigenpolarizations of THz light for InSb in longitudinal magnetic field. We label the two circular polarizations as cyclotron resonance active (CRA) and cyclotron resonance inactive (CRI). The dielectric permittivity tensor is diagonal in this eigenpolarization basis and its components can be computed as [1]

$$\epsilon_{CRA} = \epsilon_\infty - \frac{\omega_p^2}{\omega(\omega + i\gamma - \omega_c)} + \epsilon_{ph}, \tag{S1}$$

$$\epsilon_{CRI} = \epsilon_\infty - \frac{\omega_p^2}{\omega(\omega + i\gamma + \omega_c)} + \epsilon_{ph}\ , \tag{S2}$$

where the constant ϵ_∞ represents the high-frequency background permittivity, $\omega_p = ne^2/(m^*\epsilon_0)$ is the plasma frequency determined by the carrier density n and the effective mass m^*, γ is the scattering rate of charge carriers, and the $\omega_c = eB/m^*$ is the electron cyclotron frequency. ϵ_{ph} describes the phonon contribution to the permittivity given by Eq. (9) in the main text. We use equations (S1) – (S2) to compute the refractive indices $n_{CRA/CRI} = \sqrt{\epsilon_{CRA/CRI}}$ for the two eigenpolarizations and the transmission coefficients

$$t_{CRA/CRI} = \frac{4n_{CRA/CRI}}{(1 + n_{CRA/CRI})^2}\exp\left[in_{CRA/CRI}\omega d/c\right], \tag{S3}$$

where d is the thickness of InSb and c is the speed of light in vacuum. The Faraday rotation and ellipticity are calculated according to

$$\theta = (\arg(t_{CRA}) - \arg(t_{CRI})), \tag{S4}$$

$$\eta = \frac{|t_{CRA}| - |t_{CRI}|}{|t_{CRA}| + |t_{CRI}|}. \tag{S5}$$

We use equations (S1) – (S5) to fit the experimental data shown in Fig. 4(a) in the main text. We fit both the measured polarization rotation and ellipticity at the same time. The variables ϵ_∞, ω_p, γ, and the magnetic field B serve as fitting parameters. The result of the fit is shown in **Figure**

S1 below. This fit is achieved with the parameter values $\epsilon_\infty = 9.5$, $\omega_p = 0.35$ THz, $\gamma = 0.59$ THz, and $B = -0.18$ T.

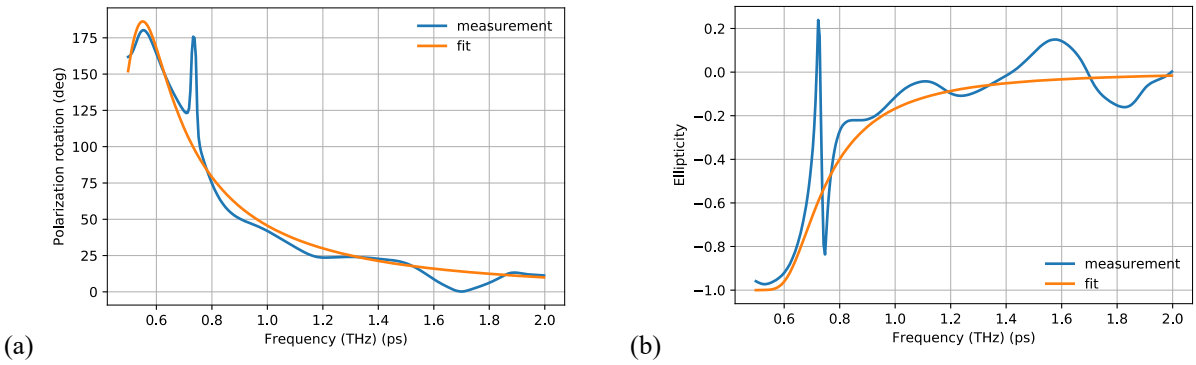

(a) (b)

Figure S1: Measured and calculated polarization rotation and ellipticity in magnetic field. Measurement was performed at 180 K temperature and magnetic field of -0.125 T.

2. Numerical simulations of the hybrid bilayer gammadion metamaterial

In our numerical simulations, we use the permittivity tensor given by equations (6) – (9) in the main text with InSb parameters at 180 K temperature that are equal to[2] $\omega_p/2\pi = 0.35\ THz$, $\gamma = 1.05\ THz$, $\epsilon_\infty = 25$ and $m^* = 0.014m_0$. **Figure S2** shows the permittivity components ϵ_{xx} and ϵ_{xy} as the magnetic field increases from $B = 0$ to $0.2\ T$. Using the above parameters, the cyclotron resonance frequency is given by $f_c = \omega_c/2\pi \approx 2 \cdot B$ THz, which matches very well with the peak of $Re(\epsilon_{xy})$ shown in **Figure S2(b)**.

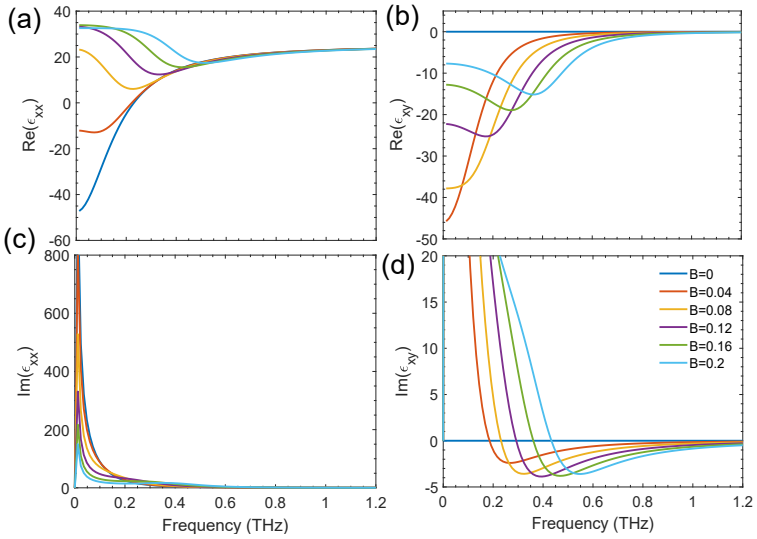

Figure S2: (a) $Re(\epsilon_{xx})$, (b) $Re(\epsilon_{xy})$, (c) $Im(\epsilon_{xx})$ and (d) $Im(\epsilon_{xy})$ are the real and imaginary parts of the dielectric permittivity of InSb used in numerical simulations.

The bilayer gammadion structure exhibits resonances at frequencies depending on its geometric size and the dielectric function of InSb. **Figures S3(a) and S3(b)** show the transmission amplitudes T_{LL}, T_{RR}, T_{LR}, T_{RL} as left-handed (L) or right-handed (R) circularly polarized waves propagating through the gammadion bilayer when no magnetic field is applied ($B = 0$). We find two resonances at $f_1 = 0.7\ THz$ and $f_2 = 0.78\ THz$ in the spectra of co-polarization transmission T_{LL} and T_{RR}, excited by the electric field and the magnetic field of the incident waves, respectively [3,4], **Figure S3(a)**. The cross-polarization transmissions, T_{LR} and T_{RL}, are close to zero as expected due to the four-fold symmetry of the gammadion structure. The ellipticity $\eta = (|T_{RR}| - |T_{LL}|)/(|T_{RR}| + |T_{LL}|)$ in **Figure S3(c)** also shows two peaks at frequencies that match with f_1 and f_2. The polarization rotation θ in **Figure S3(d)** reaches 15° between the two resonance frequencies (0.7 to 0.74 THz), indicating strong optical activity.

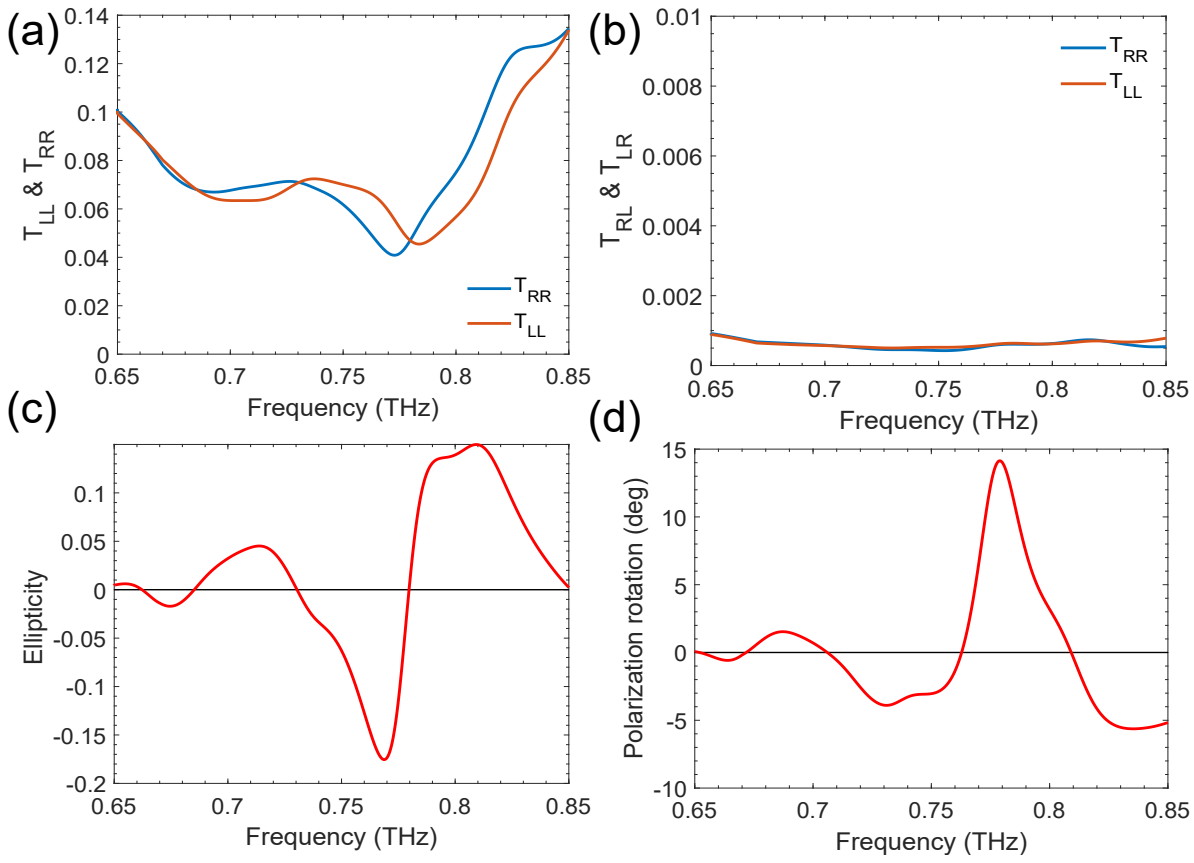

Figure S3: (a),(b) Simulated amplitude of co-polarization transmission, T_{LL} and T_{RR}, and cross-polarization transmission, T_{LR} and T_{LR}, of the bilayer gammadion hybrid metamaterial ($t_{InSb} = 500\ \mu m$). (c) Ellipticity (d) Polarization rotation. No magnetic field is applied ($B = 0$).

We find that the resonances of the gammadion bilayer change with the applied magnetic field B, as the permittivity of InSb changes with the cyclotron resonance frequency, $\omega_c = eB/m^*$. As shown in **Figure S4(a)**, the resonance in T_{LL} (indicated by the blue color) shifts towards lower frequencies and its width is also broadened when B increases. The two resonances of T_{RR}

shown in **Figure S4(b)** also shift slightly towards lower frequencies, and their strengths decrease gradually. The polarization rotation θ peaks at $f_1$and f_2 also shift towards lower frequencies as shown in **Figure S4(d),** and their strengths gradually decrease and change to the opposite sign for stronger magnetic field ($B > 0.12\ T$).

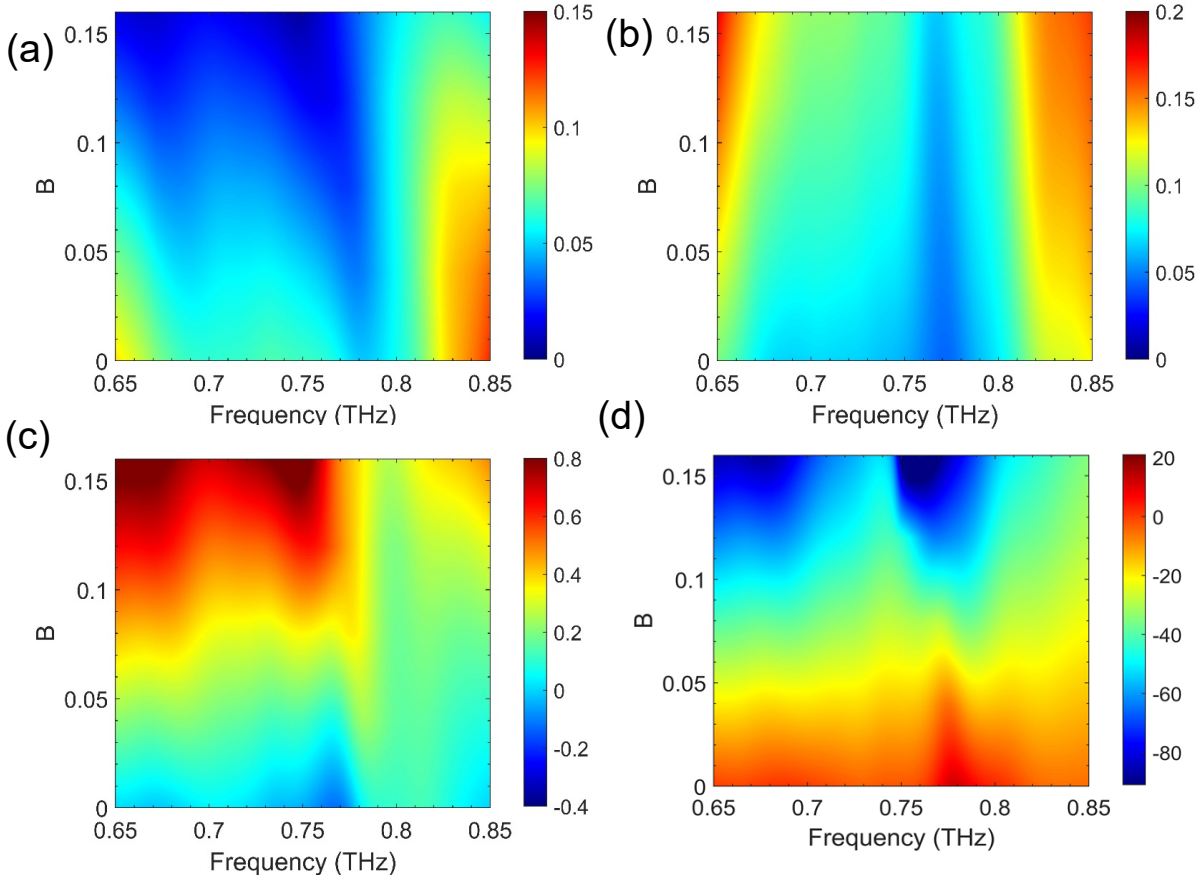

Figure S4: Simulated transmission amplitude T_{LL} (a) and T_{RR} (b) of the bilayer gammadion hybrid metamaterial with InSb layer thickness $t_{InSb} = 500\ \mu m$. (c) Ellipticity η (d) Polarization rotation θ (degree). The magnetic field increases from 0 to 0.16 T.

Figure S5(a) shows the polarization rotation θ at the resonance frequency of the bilayer gammadion hybrid metamaterial. As the magnetic field increases from $B = 0$ to $0.16\ T$, the resonance peak of θ at f_2 shifts from 0.78 THz to 0.76 THz, and the shape of the resonance changes from a peak to a dip. This change is due to the coupling of the chiral resonance of the gammadion bilayer and the cyclotron resonance of InSb, as discussed in the main text. This magneto-chiral effect can be fully controlled by varying the applied magnetic fields, which provides an opportunity to make tunable polarization control devices. As shown in **Figure S5(b)**, by varying magnetic field from -0.16 T to 0.16 T the polarization rotation can change by amount of $\Delta\theta \approx 170°$ at 0.76 THz. Unlike the polarization change induced by the Faraday effect

alone, this polarization control due to the magneto-chiral effect does not require a thick InSb layer, thereby enabling compact devices that can be integrated into optical sensors on a chip.

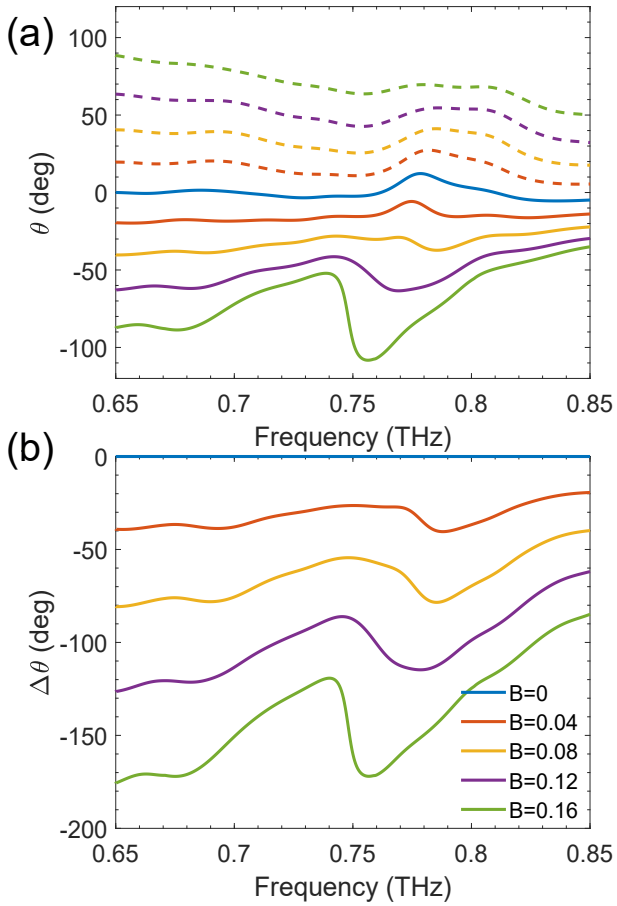

Figure S5: (a) Polarization rotation for the bilayer gammadion hybrid metamaterial on a InSb layer ($t_{InSb} = 200\ \mu m$). The solid and dash curves indicate positive and negative field, respectively. (b) $\Delta\theta = \theta(-B) - \theta(B)$. The magnetic field increases from $B = -0.16$ T to $0.16\ T$ with a step of $0.04\ T$.

3. Numerical simulations of a bare InSb substrate

Figure S6 shows the simulation results for the magneto-chiral, normal optical activity, and magneto-optical responses of a bare InSb substrate of 20 μm thickness. The magneto-chiral response and the normal optical activity are negligible, **Figure S6(a,c,d,f)**. The magneto-optical response, **Figure S6(b,e)**, results from the cyclotron motion of change carriers in the InSb substrate.

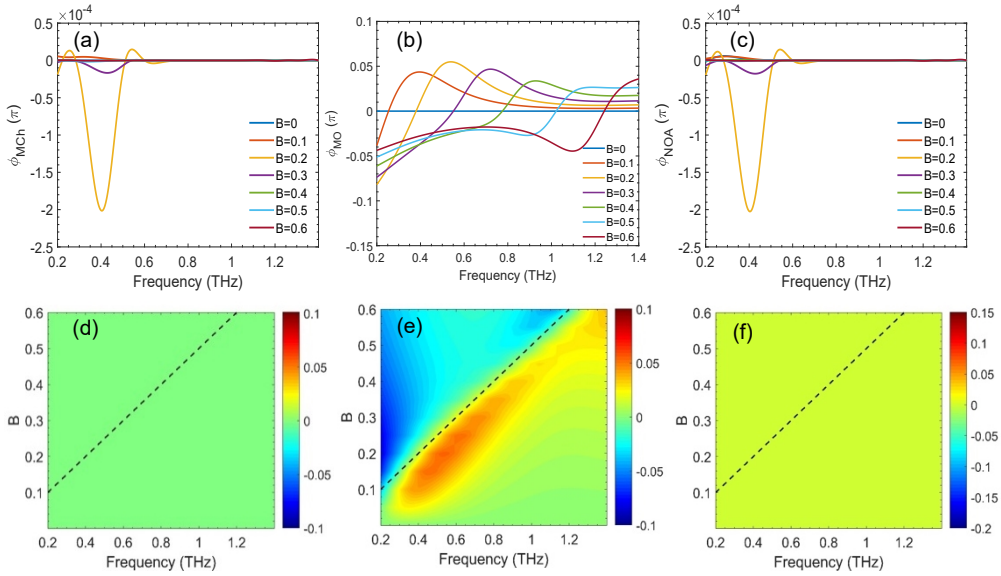

Figure S6: (a,d) Simulated magneto-chiral response of a bare InSb substrate with thickness $t_{InSb} = 20\ \mu m$. (b,e) The simulated magneto-optical response. (c,f) The simulated normal optical activity.

4. Numerical simulations of the hybrid metamaterial with only a single gammadion layer on an InSb substrate

Figure S7 shows the simulation results for a single gammadion layer on a 200-μm-thick InSb substrate with magnetic field ranging from $B = 0$ to 0.6 T. The magneto-chiral and the normal optical activity, ϕ_{MCh} and ϕ_{NOA}, are both negligible, **Figure S7(a,b)**, suggesting that a single gammadion layer exhibits vanishing chirality. The magneto-optical response ϕ_{MO} shows the resonance features due to the cyclotron resonance of carriers in the InSb substrate (**Figure S7(c)**).

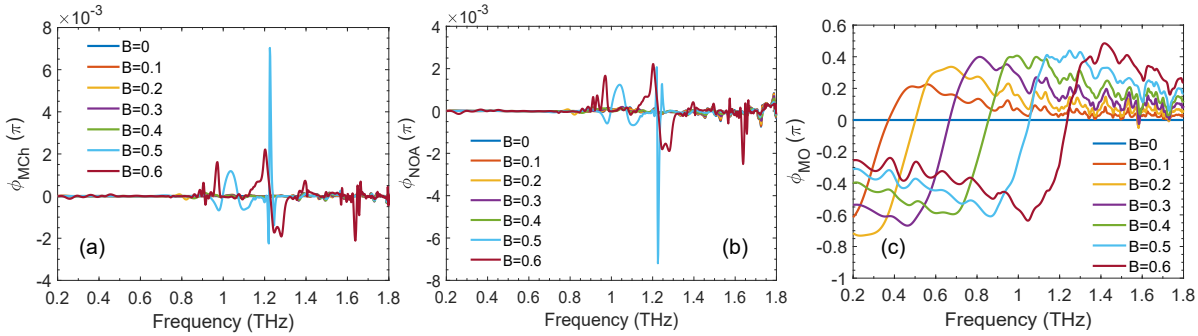

Figure S7: (a) Simulated magneto-chiral response of a single-gammadion-layer hybrid metamaterial with InSb thickness $t_{InSb} = 200\ \mu m$. (b) The simulated normal optical activity. (c) The simulated magneto-optical response.

5. Numerical simulations of the bilayer gammadion hybrid metamaterial with opposite gammadion handedness

Figure S8 shows the results of the simulations of the magneto-optical properties of our metamaterial with an opposite handedness of the gammadion bilayer. **Figure S8(a)** shows the transmission amplitude T_x in zero field and in magnetic field +/-0.16 T. The positive and negative magnetic field transmission amplitude mirrors the transmission amplitudes at opposite fields shown in **Figure 5(a)** in the main text. The polarization rotation in zero field, **Figure S8(b),** is the opposite of that in the main text in **Figure 5(b)**, as expected. In magnetic field, the overall sign of polarization rotation is the same for either handedness of the gammadion bilayer, **Figures 5(b)** and **S8(b)**. We find that the NOA phase shift, **Figure S8(f)**, changes sign upon the switching of the gammadion handedness and the sign of the MO phase shift remains unchanged, **Figure S8(e)**. The MCh phase, **Figure S8(d)**, also changes sign and offers further evidence that the MCh response near the 0.75 THz frequency behaves as the *product* of the NOA and MO effects.

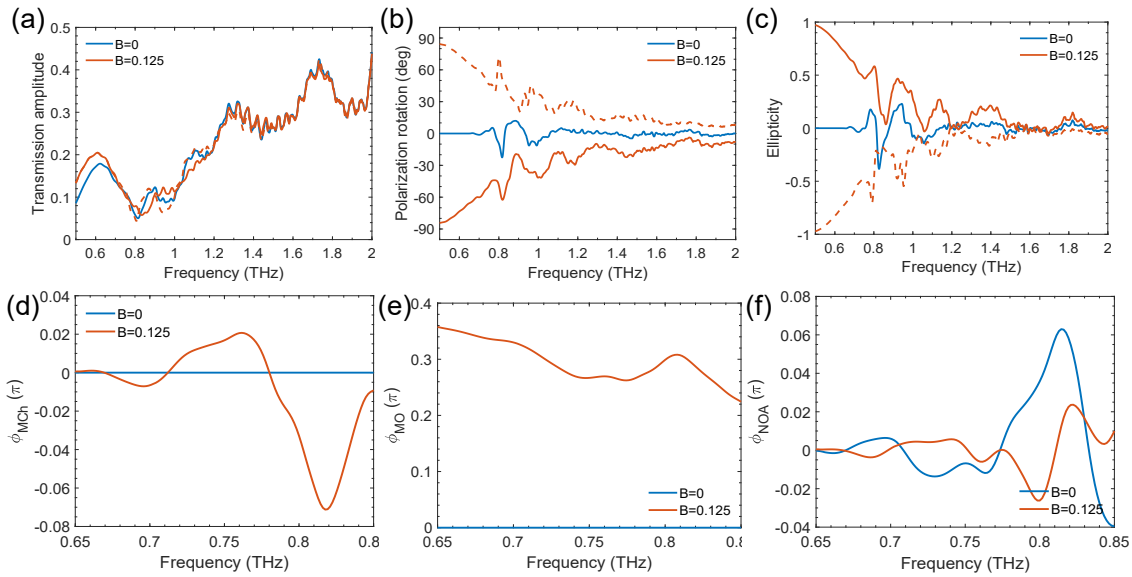

Figure S8: Simulations of a hybrid metamaterial of opposite handedness to the one described in the main text and earlier in the supplemental document. (a) Transmittance amplitude T_x in zero field and in +/-0.18 T field. (b) Polarization rotation and (c) ellipticity in zero field and in +/-0.18 T field. In panels (a)-(c), the dashed lines show the plots for the negative field values. (d) Magneto-chiral phase ϕ_{MCh}. (e) Magneto-optical phase ϕ_{MO}. (f) NOA phase ϕ_{NOA}.

6. Schematic of the experimental setup for the THz time-domain spectroscopy

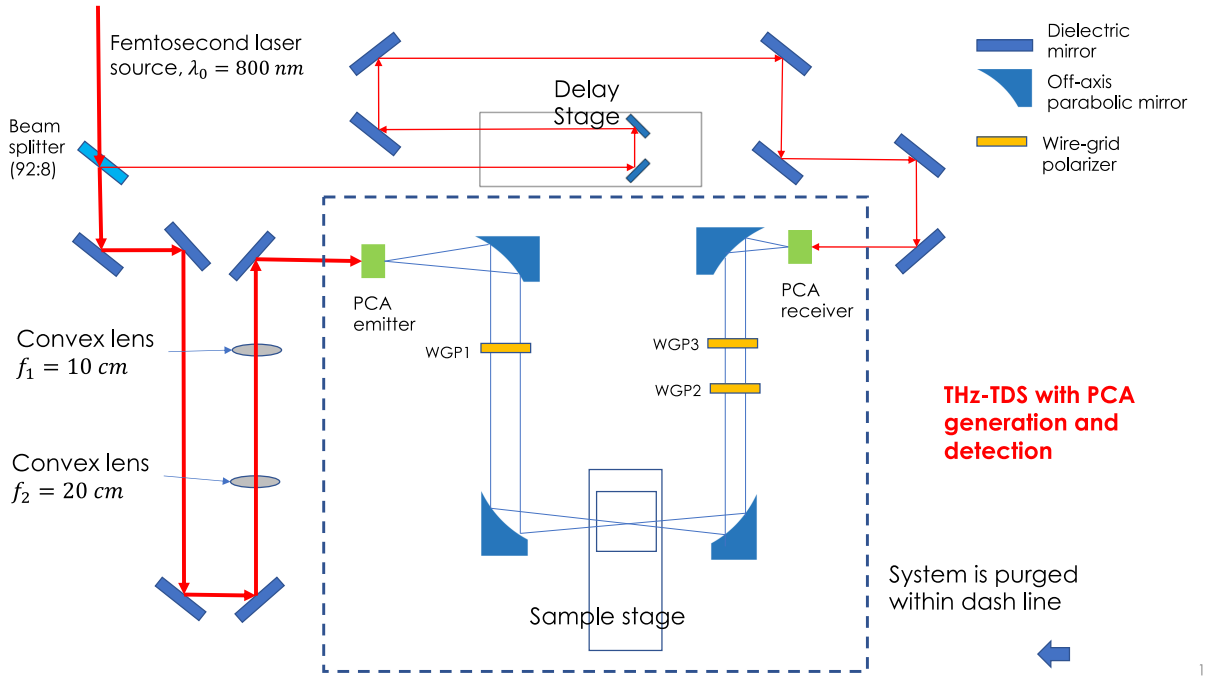

Figure S9: Schematic of a THz time-domain spectroscopy setup used in the described measurements. Top view of the measurement system.

7. Numerical simulations of the bilayer gammadions separated by an isotropic dielectric spacer

To understand the origin of the chiral response of our hybrid metamaterial and the effect of the dielectric environment, we simulated bilayer gammadions separated by an isotropic dielectric spacer with different dielectric constant ε_s. The green curves in Fig. S10(a) show the co-polarization transmission T_{LL} and T_{RR} for $\varepsilon_s = 1$, which represents the free-standing bilayer gammadions. We found that T_{LL} and T_{RR} show different amplitudes between 3.0 THz and 4 THz, indicating chiral dichroism. Correspondingly, the polarization rotation shows a sharp peak at 3.0 THz in Fig. S10(b), indicating strong optical activity. This result of the free-standing bilayer gammadion indicates that the chiral response originated from the asymmetry of the bilayer gammadion. Because of the lack of mirror symmetry, the left-handed circularly polarized (LCP) and right-handed circularly polarized (RCP) waves experience different structures as they propagate through the bilayer gammadion, and therefore leads to different amplitude and phase of T_{LL} and T_{RR}. As the dielectric constant of the spacer increases to $\varepsilon_s = 5$ and 20, the chiral dichroism and optical activities shift toward lower frequencies. Note that $\varepsilon_s = 20$ is comparable to the dielectric constant of InSb ε_{xx} in the frequency range of $f > 0.6$ THz shown in Fig. S2(a). The chiral dichroism for $\varepsilon_s = 20$ (red curves) occurs at frequencies between 0.6 THz and 1.0 THz, which agrees well with the simulation of bilayer gammadions separated by InSb shown in Fig. 5 in the main text and Fig. S3(a) in the supplemental material.

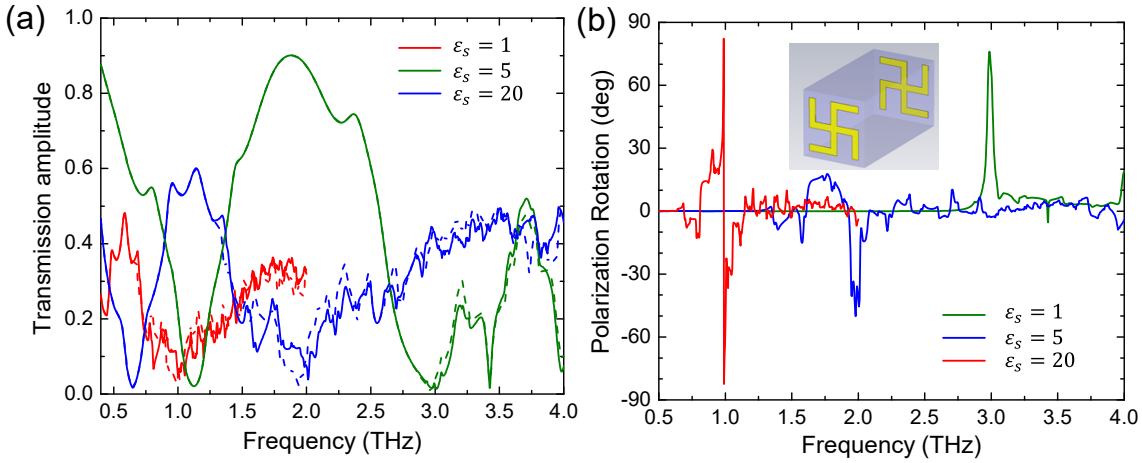

Figure S10: Simulations of bilayer gammadions separated by an isotropic dielectric spacer. (a) Transmittance amplitude T_{LL} (solid curves) and T_{RR} (dash curves) (b) Polarization rotation.

References

[1] T. Arikawa, X. Wang, A. A. Belyanin, J. Kono, *Opt Express* **2012**, *20*, 19484.

[2] S. Lin, S. Silva, J. Zhou, D. Talbayev, *Adv. Opt. Mater.* **2018**, *6*, 1800572.

[3] J. Zhou, D. R. Chowdhury, R. Zhao, A. K. Azad, H.-T. Chen, C. M. Soukoulis, A. J. Taylor, J. F. O'Hara, *Phys Rev B* **2012**, *86*, 035448.

[4] J. F. Zhou, J. F. Dong, B. N. Wang, T. Koschny, M. Kafesaki, C. M. Soukoulis, *Phys. Rev. B* **2009**, *79*, 121104.